



Limnological Analysis of Big Round Lake, Wisconsin

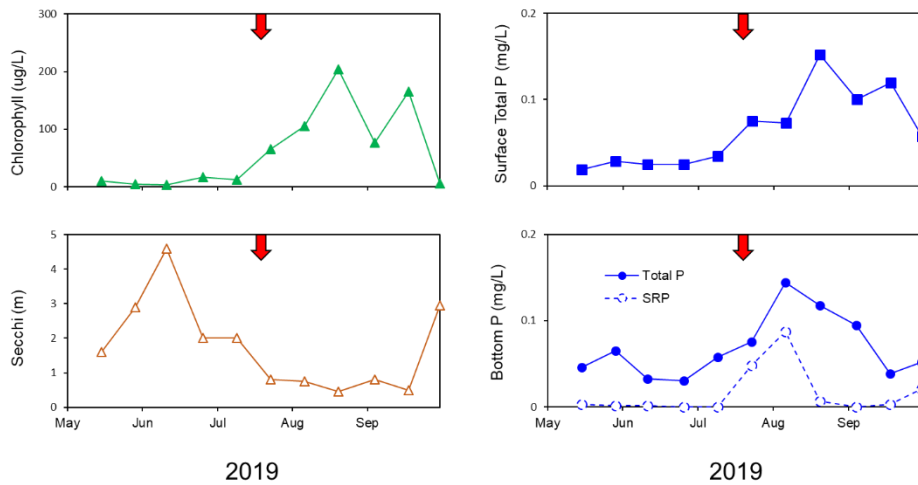


14 February 2020

University of Wisconsin - Stout
Center for Limnological Research and Rehabilitation
Menomonie, Wisconsin 54751
715-338-4395
jamesw@uwstout.edu

1.0 EXECUTIVE SUMMARY.

- Summer precipitation was above average in 2019 and severe storms with a tornado touchdown occurred near Big Round Lake on 19 July.
- Straight River inflows exhibited summer mean total and soluble reactive P concentrations of 0.068 mg/L and 0.031 mg/L, respectively, and summer loads of 221 kg and 101 kg, respectively. Soluble reactive P, directly available for algal uptake, accounted for 46% of the summer total P load from the watershed. Overall, P concentrations and loads were modest.
- Big Round Lake exhibited highly eutrophic conditions in 2019. June through September mean total phosphorus (P), chlorophyll, and Secchi transparency were 0.077 mg/L, 81.4 µg/L, and 4.89 ft, respectively. Chlorophyll concentrations peaked at over 200 µg/L in early August.

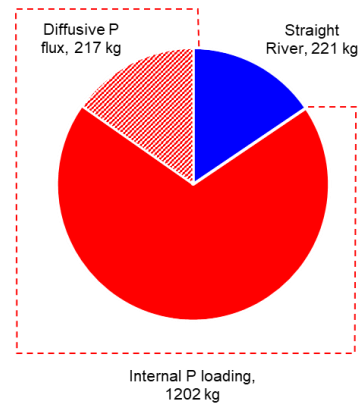


- Bottom phosphorus concentrations increased during periods of temporary stratification and anoxia, suggesting internal P loading. However, concentrations were very modest at 0.146 mg/L total P and 0.090 mg/L soluble reactive P. This pattern coincided with relatively low laboratory-derived diffusive P fluxes from sediment. The laboratory rate under anaerobic conditions was only 0.92 mg/m² d, which fell well below rates measured from other lakes in the region.
- The linear increase in lake P mass over the summer period was 1,202 kg. Straight River inflows accounted for only 16%, while laboratory-derived diffusive P flux from sediment represented only 18% of this P increase.
- Phosphorus budget discrepancies suggested the occurrence of substantial unexplained internal P loadings in 2019. The severe storms, winds, and the tornado touchdown could have somehow impacted internal P loading. Cyanobacteria as resting stages (i.e., akinetes, cysts, spores) in the sediment could have stored sediment P in cells for later growth after germination and inoculation of the water column. Wind-generated turbulence of the water column during the tornado could

have mixed germinated cyanobacteria into the water column as well as modest concentrations of hypolimnetic P that had accumulated in the bottom waters, resulting in prolific growth and bloom conditions.

- More information is needed on algal genera assemblage and historical patterns of P mass buildup in the lake to better understand potential mechanisms of internal P loading. Empirical modeling is needed to evaluate 2019 compared to other years and the lake response to internal P loading reduction.

2019 Summer P Loads



2.0 OBJECTIVES.

The objectives of these investigations were to examine the development of summer algal blooms in Big Round Lake (Table 1) in relation to P loading from the Straight River watershed and from bottom sediment during temporary anoxia. The goals of this research were to develop an estimate of summer watershed and sediment-derived internal P loading for use in P budgetary analysis and future forecasting of the impacts of internal P loading management on water quality.

3.0 METHODS.

Stratification, mixing, and bottom dissolved oxygen dynamics

Data logging thermistors (HOBO temperature loggers, Onset, Corp) were deployed in the deepest region of the lake (Fig. 1) at 0.5-m intervals from the surface to near bottom to record temperature at 1-hour intervals between June and October 2019, in order to quantify the frequency of occurrence of stratification and mixing periods. A YSI 6600 data sonde equipped with precalibrated probes was deployed in the lake approximately 0.25 to 0.50 m above the sediment-water interface to examine seasonal changes in in situ variables to quantify periods of temporary bottom anoxia and high pH that might be regulating diffusive P flux from sediments in Big Round Lake. However, the data sonde was deployed too close to the sediment-water interface and sunk into the soft sediments shortly after deployment. Fortunately, biweekly in situ monitoring captured periods of bottom anoxia for use in evaluating periods of potential diffusive P flux from sediments.

Schmidt stability (S ; g-cm/cm²) was calculated as:

$$S = 1/A \int_0^{z_m} (z - z_g)(\rho_z - \rho_g) dz$$

where A = surface area (m^2), z_m = maximum depth (m), z = depth at stratum z , z_g = depth of the center of mass or ρ_g , and ρ_z = the density of water (kg/m^3) at depth z (Idso 1973). ρ_g was calculated as:

$$\rho_g = 1/V \int_0^{z_m} V_z \rho_z dz$$

where V is lake volume (m^3) and V_z is the volume at depth z . Schmidt stability represented the amount of work (in the form of wind power, motor boat activity, etc) required to completely mix a water body (without loss of gain in heat content) that is stratified due to vertical differences in water density. Higher stability values were indicative of strong stratification and greater work required to disrupt stratification. Conversely, lower stability values were indicative of weak stratification and less work required to disrupt stratification.

In-lake and tributary monitoring

Water samples for limnological variables were collected biweekly between May and early October at the same station in the deepest portion of the lake (Fig.1). An integrated sample was collected over the upper 2-m for analysis of total phosphorus and chlorophyll a. An additional discrete sample was collected within 0.5 m of the sediment surface for analysis of total and soluble reactive P. Secchi transparency and in situ measurements (temperature, dissolved oxygen, pH, and conductivity) were collected on each date. In situ measurements were recorded at 0.5-m intervals using a YSI 6600 data sonde (Yellow Springs Instruments, Inc., Yellow Springs, OH) that was precalibrated with known pH buffers and independent Winkler titrations for dissolved oxygen (APHA 2011).

Sampling stations established on the Straight River at Hwy 48 (upstream) and 70th St. (downstream) were sampled biweekly for analysis of total P and SRP between May and early October. The original upstream station was to be located at 270th St. However, road and bridge work were being conducted and a debris dam was impacting flow velocity at that site (Fig. 2), necessitating relocation of this station to Hwy 48. A continuous water

level monitor (HOBO, Onset Corp) was deployed on the Straight River at Hwy 48 to record stage at 25 min intervals. Volumetric flow was measured at biweekly intervals using a flow velocity probe (Marsh McBirney Flo-mate). A stage-flow relationship was developed to estimate continuous flow (m^3/s). A water level monitor (HOBO, Onset Corp) was also deployed in the lake to monitor changes in pool elevation.

Samples for total P were digested with potassium persulfate prior to analysis (APHA 2011). Samples for soluble reactive P were filtered immediately in the field using a 0.45 μm pore size syringe filter. Phosphorus was analyzed on a Perkin-Elmer UV-VIS Lambda 25 Spectrophotometer using the ascorbic acid method (APHA 2011). Samples for chlorophyll analysis were filtered onto a type A/E glass fiber filter, extracted in 90% acetone overnight in the freezer, and analyzed fluorometrically using a TD 300 fluorometer (Turner Designs). Phosphorus loading from the Straight River was estimated using the computer program FLUX (Walker 1996).

Laboratory-derived rates of P release from sediment

Sediment in Big Round Lake may represent a potentially significant internal source of P recycling to the overlying water column via diffusion from porewater to the overlying water column, contributing to cyanobacterial blooms under P-limited conditions particularly when watershed point and nonpoint source loadings are nominal. During periods of temporary stratification and establishment of bottom water hypoxia or anoxia, P chemically adsorbed or precipitated to metal compounds (i.e., iron oxyhydroxides; $\text{Fe}(\text{OOH})\sim\text{P}$) can diffuse from sediment into the overlying water column as a result of reduction reactions under anaerobic conditions (Mortimer 1971, Boström 1984, Nürnberg 1988). Under aerobic conditions at the sediment-water interface, P is typically bound to $\text{Fe}(\text{OOH})$ within a thin (often 1 mm or less in thickness) surface oxidized microzone. Although rates of diffusive P flux are constrained by Fe binding under aerobic conditions, and much lower to negligible compared to fluxes under anaerobic conditions, contributions can still play a potential role in driving cyanobacterial production under P-limited conditions. Thus, information was needed on sediment diffusive P flux

contributions (i.e., internal P loading) in Big Round Lake to better understand and quantify the P budget.

Sediment cores were collected at the WQ sampling station in Big Round Lake for determination of diffusive P flux from sediment under controlled laboratory conditions. Cores were carefully drained of overlying water in the laboratory and the upper 10 cm of sediment were transferred intact to a smaller acrylic core liner (6.5-cm dia and 20-cm ht) using a core remover tool. Surface water collected from each lake was filtered through a glass fiber filter (Gelman A-E), with 300 mL then siphoned onto the sediment contained in the small acrylic core liner without causing sediment resuspension. They were placed in a darkened environmental chamber and incubated at a constant temperature of ~20 °C to reflect summer conditions. The Eh environment in the overlying water was controlled by gently bubbling air (aerobic) or nitrogen-CO₂ (anaerobic) through an air stone placed just above the sediment surface in each system. Bubbling action insured complete mixing of the water column but not disrupt the sediment. The pH of systems subjected to aerobic conditions were controlled by bubbling with air (pH ~ 8.0 to 8.5) or CO₂-free air (pH ~ 9.0-9.5). A total of 9 cores were collected for assessment of diffusive P flux from sediment.

Water samples for soluble reactive P were collected from the center of each system using an acid-washed syringe and filtered through a 0.45 µm membrane syringe filter. The water volume removed from each system during sampling was replaced by addition of filtered lake water preadjusted to the proper oxidation-reduction condition. These volumes were accurately measured for determination of dilution effects. Soluble reactive P was measured colorimetrically using the ascorbic acid method (APHA 2011). Rates of P release from the sediment (mg/m² d) were calculated as the linear change in mass in the overlying water divided by time (days) and the area (m²) of the incubation core liner. Regression analysis was used to estimate rates over the linear portion of the data.

Evaluation of sediment P characteristics

The objectives of this task were to quantify vertical variations in sediment textural characteristics and mobile P fractions involved in sediment internal P loading to the overlying water column. Sediment cores were sectioned at 1-cm intervals over the upper 6 cm and 2-cm intervals thereafter for analysis of sediment physical-textural characteristics and P fractions. Sediment sections were analyzed for moisture content, sediment density, organic matter content, loosely-bound P, iron-bound P, labile organic P, and aluminum-bound P. Subsamples were dried at 105 °C to a constant weight and burned at 500 °C for determination of moisture content, sediment density, and organic matter content (Håkanson and Jensson 2002). Phosphorus fractionation were conducted according to Psenner and Puckso (1988) and Hjieltjes and Lijklema (1980) for the determination of ammonium-chloride-extractable P (1 M NH₄Cl; loosely-bound P), bicarbonate-dithionite-extractable P (0.11 M BD; iron-bound P), and sodium hydroxide-extractable P (0.1 N NaOH; Aluminum-bound and labile organic P).

The loosely-bound and iron-bound P fractions are readily mobilized at the sediment-water interface under anaerobic conditions that result in desorption of P from bacterially-reduced iron compounds (i.e., Fe⁺³ to Fe⁺²) in the sediment and diffusion into the overlying water column (Mortimer 1971, Boström 1984, Nürnberg 1988). The sum of these fractions are referred to as redox-sensitive P (i.e., redox-P; the P fraction that is active in P release under anaerobic and reducing conditions). In addition, labile organic P (LOP) can be converted to soluble P via bacterial mineralization (Jensen and Andersen 1992) or hydrolysis of bacterial polyphosphates to soluble phosphate under anaerobic conditions (Gächter et al. 1988; Gächter and Meyer 1993; Hupfer et al. 1995). The sum of redox-P and LOP is collectively referred to a biologically-labile P. This fraction is generally active in recycling pathways that result in exchanges of phosphate from the sediment to the overlying water column and potential assimilation by algae.

4.0 RESULTS.

Hydrology and watershed phosphorus loading

Annual precipitation (measured at Amery WI) was above normal in 2019 compared to the average since 1980 (Fig. 3). In addition, severe storms, high winds, and tornado touchdowns occurred in the vicinity of Big Round Lake on 19 July, resulting in local precipitation in excess of 2 inches (Fig. 4). Local precipitation (measured at Amery and Luck WI) in excess of 1 inch occurred in early and mid-May, mid- and late July, mid- and late August, and late September (Fig. 4).

Straight River inflow at Hwy 48 and Big Round Lake pool volume fluctuated as a result of local storms, increasing to peaks particularly in response to storms exceeding 1 inch (Fig. 4). A series of precipitation events between mid-August and early October resulted in numerous peaks in flow and increases in pool elevation. Direct precipitation onto the lake and Straight River inflows accounted for ~ 43% and 57% of the measured water income to the lake, respectively (Table 2). Theoretical residence time during the June-September period averaged 1.42 y, typical for large glacially-formed lakes in the region.

Total P and SRP concentrations in the Straight River inflow to Big Round Lake were maximal in mid-May at 0.154 mg/L and 0.054 mg/L, respectively (Fig. 5). Concentrations declined between June and September, ranging between 0.054 mg/L and 0.085 mg/L total P and 0.019 mg/L and 0.046 mg/L SRP. The flow-averaged summer (June-September) concentration was 0.068 mg/L total P and 0.031 mg/L SRP (Table 3). SRP accounted for 46% of the total P in the Straight River inflow.

Big Round Lake outflow total P was less than Straight River inflow total P between mid-May and early July, indicating a portion of the inflow total P was retained in the lake, probably as particles that settled to the lake bottom. SRP concentrations were lower and near detection limits in the outflow compared to much higher concentrations in the inflow, suggesting uptake by algae for growth. Thus, another portion of the retained total

P was in particulate organic form as algal biomass during the mid-May to early July period.

Between mid-July and early September, outflow total P was often greater than the Straight River inflow (Fig. 5). This pattern suggested that algae were assimilating additional P from internal sources (i.e., the sediment) for growth and a portion of this algal biomass was discharged from the lake. Outflow P > inflow P was strong indication of the occurrence of internal P loading (Nürnberg 2009). Low outflow SRP concentrations relative to the inflow further indicated that algae were also assimilating watershed-derived SRP in addition to SRP originating from internal P loads during this period.

Measured and predicted watershed P loading from the Straight River are shown in Figure 6. Overall, the Straight River watershed delivered 221 kg of total P and 101 kg of SRP between June and September 2019 (Table 3).

Lake limnological conditions

The temperature array deployed in Big Round Lake captured several periods of temporary stratification and mixing throughout the summer of 2019 (Fig. 7). Periods of temporary stratification developed in late May-early June, late June, early July, and early to mid-August. Several periods of surface water cooldown and heat loss as a result of cold fronts passing through the area disrupted temporary stratification and resulted in either partial mixing and expansion of the epilimnion or nearly complete mixing and lake turnover. Mixing and potential entrainment of internal P loading occurred in mid-June, late July, and Mid-August. In particular, lake temperatures cooled and partial mixing occurred during the period of severe storms and tornado touchdowns on 19 July 2019.

Bottom anoxia (defined as dissolved oxygen < 1 mg/L and determined from biweekly in situ monitoring) developed as a thin layer above the sediment-water interface in early July 2019, shortly after strong stratification developed (Fig. 8). Although severe storms and winds associated with tornado touchdowns caused extensive water column mixing in

late July, complete turnover apparently did not occur and bottom anoxia was not disrupted. However, vertical expansion of the anoxic layer appeared to be suppressed as the extent of bottom anoxia remained at 0.25 m above the sediment-water interface after the storm period. Bottom anoxia expanded to the 4.5-m depth during a period of strong stratification in early August. Hypoxic conditions (defined as Nearly complete water column turnover in mid- to late August reoxygenated the entire water column. Thus, bottom anoxia (< 1 mg/L) and the potential for anaerobic diffusive P flux from sediment occurred for ~ 1.5 months in 2019. The Anoxic Factor (Nürnberg 1995) was ~ 18 days.

Bottom total P and SRP concentration were between May and early July, coinciding with aerobic conditions near the sediment-water interface (Fig. 9). Bottom P increased after the development of anoxic conditions and exhibited concentration maxima of 0.146 mg/L total P and 0.090 mg/L SRP on 7 August. These concentration peaks were modest compared to those observed in deeper eutrophic lakes that exhibit strong stable stratification and hypolimnetic anoxia throughout the summer. For instance, hypolimnetic P concentrations can exceed 1 mg/L by late summer in these systems. Bottom P concentrations declined in Big Round Lake in conjunction with water column turnover and reintroduction of dissolved oxygen in mid-August. Nevertheless, seasonal patterns indicated internal P loading and the development of elevated hypolimnetic P concentrations occur rapidly during periods of temporary stratification and bottom anoxia.

Surface chlorophyll concentrations were very low (< 15 $\mu\text{g/L}$) in conjunction with low total P (< 0.035 mg/L) between late May and early July 2019 (Fig. 9). Secchi transparency increased to the lake bottom (> 4.5 m) on 11 June and was generally > 2 m between late May and early July. Chlorophyll and surface total P concentrations increased rapidly and linearly between late July and mid-August, shortly after the severe storm period of 19 July. The maximum chlorophyll and surface total P concentrations were 207 $\mu\text{g/L}$ and 0.153 mg/L, respectively, on 21 August. Secchi transparency declined to < 0.5 m in conjunction with the algal bloom.

Strong regression relationships between surface chlorophyll and total P indicated incorporation of P into algal biomass and P-limitation of growth and bloom development (Fig. 10). Thus, reducing P loading to Big Round Lake should result in lower chlorophyll concentrations and deeper Secchi transparencies. Overall, peak chlorophyll and surface total P concentrations in August 2019 were among the highest observed when compared to historical monitoring (Fig. 11).

Mean summer limnological trophic state variables reflected eutrophic conditions in Big Round Lake 2019 (Table 4). Mean total P was 0.077 mg/L, mean chlorophyll was 81 ug/L, and mean Secchi transparency was 4.89 ft.

Sediment characteristics and diffusive phosphorus flux

Soluble phosphorus concentration increased linearly in the overlying water column with respect to days of incubation under both anaerobic (i.e., no dissolved oxygen) and aerobic (i.e. dissolved oxygen availability) conditions (Fig. 12). Diffusive P fluxes were much greater under anaerobic conditions at a mean $0.92 \text{ mg/m}^2 \text{ d}$ (± 0.12 standard error, SE, Table 5) suggesting release of P from reduced iron (Fe^{2+}). Although much lower, aerobic diffusive P fluxes were detectable at a mean $0.35 \text{ mg/m}^2 \text{ d}$ (± 0.08 SE, Table 5). The mean anaerobic diffusive P flux for Big Round Lake was very modest and fell below the lower 25% quarter when compared to other lakes in the region (Fig. 13). In contrast, the mean aerobic diffusive P flux was relatively high compared to other lakes in the region, falling near the median (Fig. 13).

Sediment moisture content was very high in the upper 5-cm sediment layer and exceeded 95% near the sediment core surface, suggesting very flocculent sediment (Fig. 14).

Organic matter content was also high in the upper 5-cm sediment layer and approached 40% in the surface sediment layer. This pattern may be attributable to algal and macrophyte remains concentrated near the sediment surface.

Biologically-labile (i.e., subject to recycling pathways leading to internal P loading) P concentrations exhibited maxima in the upper 5-cm layer and declined to lower concentrations below the 5-cm sediment depth (Fig. 14). Surface concentration bulges reflect the buildup of potentially mobile P in excess of burial, a pattern typically observed in eutrophic lake systems exhibiting internal P loading and low P burial efficiency (Carey and Rydin 2011, Rydin et al. 2011).

Labile organic P was the dominant biologically-labile fraction in the upper 5-cm sediment layer at 70% (Fig. 15). The concentration was also high relative to sediment cores collected in other lakes in the region (Fig. 16). Iron-bound P was the next dominant fraction, accounting for 27% of the biologically labile P. The iron-bound P concentration was moderate in Big Round Lake and fell within the lower 25% quartile compared to other lakes (Fig. 16). Overall, redox-P concentrations (i.e., the sum of loosely-bound and iron-bound P) in the upper 5-cm sediment layer of Big Round Lake fell within the lower 25% quartile. Since this P fraction is strongly related to anaerobic diffusive P flux (Nürnberg 1988), the modest concentration suggested that diffusive P flux was also moderate. Predicted P flux, based on redox-P versus anaerobic diffusive P flux regression models developed by Nürnberg (1988), were $\sim 1.2 \text{ mg/m}^2 \text{ d}$ based on $11 \text{ } \mu\text{g/g}$ FW redox P. The predicted value was similar to anaerobic diffusive fluxes measured for Big Round Lake.

Summer phosphorus mass balance and budget

Lake-wide internal P loading during the summer was estimated using 3 approaches to obtain ranges for comparison with Straight River P inputs and to gain better insight into possible linkages with cyanobacteria bloom development; P mass balance, laboratory-derived diffusive P fluxes, and sediment core P profiles.

P mass balance - Net internal P loading derived from the summer P mass balances was estimated by difference from the equation,

$$\Delta P_{\text{lake storage}} = (P_{\text{external load}} - P_{\text{outflow}}) \pm P_{\text{net internal load}} \quad 1),$$

where $\Delta P_{\text{lake storage}}$ = the change in lake P mass over a defined summer period (kg), $P_{\text{external load}}$ = the P mass input to the lake from Straight River (kg), P_{outflow} = the P mass that was discharged from the lake (kg), and $P_{\text{external load}} - P_{\text{outflow}}$ = net retention of external P loads ($P_{\text{net retention}}$, kg), $P_{\text{groundwater}}$ (P inputs from groundwater seepage into the lake) were assumed to be negligible based on analysis of the hydrologic budget. $P_{\text{lake storage}}$ was calculated as,

$$\Delta P_{\text{lake storage}} = \sum_{i=0}^n P_{\text{concentration}} \cdot \text{Volume} \quad 2),$$

where $P_{\text{concentration}}$ = the TP concentration (mg/L or g/m³) and Volume = the water volume (m³) at depth i (m). The product of these variables (kg) for each depth layer was summed over the entire water column (n = maximum depth, m) to estimate $P_{\text{lake storage}}$.

$P_{\text{lake storage}}$ was relatively low and constant from May to late June then increased ~ linearly between July and mid-September (Fig. 18). The maximum occurred on 21 August 2019 in conjunction with peaks in chlorophyll (Fig. 9), suggesting incorporation of P as algal biomass. Net internal P loading, estimated from equation 1, was 1,202 kg/summer (Table 6). By comparison, $P_{\text{external load}}$ was only 221 kg/summer.

Laboratory-derived diffusive P flux - Summer internal P loading was estimated from laboratory-derived diffusive P as,

$$\text{Internal P load} = \sum_{t=0}^n (\text{Anaerobic P flux} \bullet \text{anoxic area}) + (\text{Aerobic P flux} \bullet \text{oxic area}) \quad 3),$$

where the anaerobic diffusive P flux = 0.92 mg/m² d, the aerobic diffusive P flux = 0.35 mg/m² d (Table 5), and the anoxic or oxic areas were areas that were seasonally anoxic and oxic on each sampling date between June and the end of September. Surprisingly, internal P loading estimated from laboratory-derived P fluxes were only 217 kg/summer,

accounting for only 18% of the internal P loading rate calculated from P mass balance (Table 6).

Sediment core profiles – Phosphorus concentration maxima near the sediment surface can represent an imbalance between P deposition and P burial (Mooseman et al. 2006, Carey and Rydin 2011, Rydin et al. 2011). Positive differences between surface P and buried P concentrations reflect a long-term average annual internal P loading rate. Reasons for poor P burial (i.e., sediment P that has been buried with new sediment and is no longer active in recycling and internal P loading) efficiency include annual recycling of P into the water column by diffusive flux, uptake by cyanobacteria for growth, deposition of cells back to the sediment, breakdown of organic P to PO₄-P, and binding back to iron oxyhydroxides (James 2017). Thus, internal P loading coupled with cyanobacterial uptake can be responsible for promoting and maintaining high P concentrations in the surface layer of eutrophic lake sediments.

Annual long-term internal P loading was approximated from P profiles in the sediment by comparing P concentration differences in surface sediment layer and in the buried layer (Rydin et al. 2011). From Figure 20, sediment biologically-labile (i.e., subject to internal P loading) P concentrations were high near the sediment surface at 1.095 mg/g and reflected newly deposited sediment (gross P deposition in Figure 19). Concentrations declined and were relatively constant below the 6-cm depth at 0.369 mg/g, indicating no further change and burial from further activity and recycling pathways (i.e., the stabilization depth Figure 19). Using a relatively constant sedimentation rate since 1960 of ~ 0.011 g/cm² d (Garrison and La Liberte 2007), the long-term deposition, burial, and internal P loading rate were approximated as,

P deposition (kg/y) = Surface P concentration × sedimentation rate

P burial (kg/y) = P concentration below 6 cm × sedimentation rate

P internal loading (kg/y) = P deposition – P burial (Table 7).

The long-term core-derived internal P loading rate was 328 kg/y, higher than the estimated laboratory diffusive P flux of 217 kg/y, but still much lower than the internal P loading rate of 1,202 kg/y estimated by P mass balance (Table 6).

The comparison of three independently estimated internal P loading rates suggested several insights and uncertainties regarding P recycling mechanisms driving excessive algal blooms in Big Round Lake. First, internal P loading estimated by P mass balance represented 84% while the Straight River watershed accounted for only 16% of the measured summer P inputs to the lake. Second, diffusive P flux accounted for only 18% of the P mass balance rate, suggesting other internal P loading processes were important in 2019. Third, the core-derived internal P loading rate, while higher, only accounted for 27% of the P mass balance in 2019 and also did not explain the high rate estimated from P mass balance. Thus, a large portion of the 2019 summer P mass balance residual of 1,202 kg was not explained by typically-invoked flux of P from sediment.

The summer of 2019 was unusual in that tornadoes and potentially high winds could have somehow exacerbated internal P loading compared to other years. Phosphorus started accumulating in the anoxic hypolimnion before the tornado event (Fig. 9). Although concentrations were modest, mixing and entrainment of soluble P into the epilimnion as a result of tornadic winds could have stimulated cyanobacteria growth in August. Another possible contributing (but unlikely) mechanism of enhanced internal P loading could have been resuspension of shallow sediments into the water column during the tornado event. Resuspended sediment particles could have released P into the water column for uptake by cyanobacteria.

Finally, many cyanobacteria form resting stages as akinetes or spores that reside in the sediment and germinate under optimal environmental conditions. These resting stages may directly assimilate sediment P in excess of growth requirements and develop extensive blooms when mixed into the water column (Istvanovics et al. 1993, 2000; Pettersson et al. 1993; Perakis et al. 1996; Cottingham et al. 2015). Extensive water column mixing during the tornado event, could have mixed germinating cyanobacteria

into the water column. They used the stored cellular P that was derived from the sediment and assimilated any additional entrained bottom P for growth to bloom proportions after the tornado. This latter hypothesis is the most plausible, but more information is needed on the algal species assemblage in Big Round Lake to verify the possibility of akinete-forming cyanobacteria.

4.0 CONCLUSIONS AND RECOMMENDATIONS

High rates of internal P loading and the development of extensive algal blooms in Big Round Lake during the summer of 2019 could be anomalous and related to extreme summer weather patterns and the occurrence of tornadic events. Nevertheless, internal P loading, much of which is not explained by typical anoxic diffusive P flux from sediment, dominated the summer P budget and appeared to be a significant source of P to the lake. If so, internal P loading can be managed via several tools, included aluminum sulfate. However, the cost of management will likely be very expensive, on the order of millions of dollars, due the size of the lake and large sediment surface area.

More information is needed to better understand the role of internal P loading in the lake and to place into context seasonal algal bloom dynamics in 2019 versus other years.

Recommendations include:

1. An evaluation of historical patterns in summer concentrations of total P, chlorophyll, and Secchi transparency for comparison with lake response during the unusual tornado event of 2019. Were summer mean lake WQ variables (total P, chlorophyll) higher in 2019 versus other years?
2. An empirical modeling approach using historical and current WQ conditions to predict lake response to internal P loading reduction and evaluate overall WQ goals for the lake. Will management of internal P loading reduce lake total P and chlorophyll to target levels (as per WisCalm 2019) and meet WQ goals.
3. A better understanding of algal genera and potential cyanotoxin development in the lake. Water samples could be preserved for algal identification. Do toxin-

- forming cyanobacteria develop blooms in the lake? Do they form resting stages and inhabit the sediment, with the potential for directly assimilating and storing this P for later growth?
4. Further measurement of diffusive P fluxes and surface sediment P concentrations to verify and better understand the role sediment diffusive P flux in the overall summer P budget of the lake. Some spatial sediment core analysis in other regions of the lake would provide a clearer picture of sediment P distribution and flux.

5.0 REFERENCES.

APHA (American Public Health Association). 2011. Standard Methods for the Examination of Water and Wastewater. 22th ed. American Public Health Association, American Water Works Association, Water Environment Federation.

Boström B. 1984. Potential mobility of phosphorus in different types of lake sediments. *Int Revue Ges Hydrobiol* 69:457-474.

Carey C, Rydin E. 2011. Lake trophic status can be determined by the depth distribution of sediment phosphorus. *Limnol Oceanogr* 56:2051-2063.

Cottingham KL, Ewing HA, Greer ML, Carey CC, Weathers KC. 2015. Cyanobacteria as biological drivers of lake nitrogen and phosphorus cycling. *Ecosphere*. 6:1–19.

Gächter R., Meyer JS, Mares A. 1988. Contribution of bacteria to release and fixation of phosphorus in lake sediments. *Limnol Oceanogr* 33:1542-1558.

Gächter R, Meyer JS. 1993. The role of microorganisms in mobilization and fixation of phosphorus in sediments. *Hydrobiologia* 253:103-121.

Garrison PK & LaLiberte G. 2007. Paleoecological study of Big Round Lake, Polk County. Wisconsin Department of Natural Resources. October 2007.

Håkanson L, Jansson M. 2002. Principles of lake sedimentology. The Blackburn Press, Caldwell, NJ USA

Hjieltjes AH, Lijklema L. 1980. Fractionation of inorganic phosphorus in calcareous sediments. *J Environ Qua.* 8: 130-132.

Hupfer M, Gächter R., Giovanoli R. 1995. Transformation of phosphorus species in settling seston and during early sediment diagenesis. *Aquat Sci* 57:305-324.

Istvanovics V, Pettersson K, Rodrigo MA, Pierson D, Padisak J, Colom W. 1993. *Gloeotrichia echinulata*, a colonial cyanobacterium with a unique phosphorus uptake and life strategy. *J Plankton Res.* 15:531–552.

Istvanovics V, Shafik HM, Presing M, Juhos S. 2000. Growth and phosphate uptake kinetics of the cyanobacterium, *Cylindrospermopsis raciborskii* (Cyanophyceae) in throughflow cultures. *Freshwater Biol* 43:257–275.

James WF. 2017. Diffusive phosphorus fluxes in relation to the sediment phosphorus profile in Big Traverse Bay, Lake of the Woods. *Lake Reserv Manage* 33:360-368.

- Mooseman L, Gächter R, Müller B, Wüest A. 2006. Is phosphorus retention in autochthonous lake sediments controlled by oxygen or phosphorus? *Limnol Oceanogr* 51:763–771.
- Mortimer CH. 1971. Chemical exchanges between sediments and water in the Great Lakes – Speculations on probable regulatory mechanisms. *Limnol. Oceanogr* 16:387-404.
- Nürnberg GK. 1988. Prediction of phosphorus release rates from total and reductant-soluble phosphorus in anoxic lake sediments. *Can J Fish Aquat Sci* 45:453-462.
- Nürnberg GK. 1995. Quantifying anoxia in lakes. *Limnol Oceanogr* 40:1100-1111.
- Nürnberg GK. 2009. Assessing internal phosphorus load – Problems to be solved. *Lake Reserv Manage* 25:419-432.
- Perakis SS, Welch EB, Jacoby JM. 1996. Sediment-to-water blue green algal recruitment in response to alum and environmental factors. *Hydrobiologia* 318:165–177.
- Pettersson K, Herlitz E, Istvanovics V. 1993. The role of *Gloeotrichia echinulata* in the transfer of phosphorus from sediments to water in Lake Erken. *Hydrobiologia* 253: 123–129.
- Psenner R, Puckso R. 1988. Phosphorus fractionation: Advantages and limits of the method for the study of sediment P origins and interactions. *Arch Hydrobiol Biel Erg Limnol* 30:43-59.
- Rydin E, Malmaeus JM, Karlsson OM, Jonsson P. 2011. Phosphorus release from coastal Baltic Sea sediments as estimated from sediment profiles. *Est Coast Shelf Sci.* 92: 111–117.

Walker WW. 1996. Simplified procedures for eutrophication assessment and prediction: User manual. Instruction Report W-96-2, September 1996, U.S. Army Engineer Waterways Experiment Station, Vicksburg, Mississippi, USA.

Table 1. Big Round Lake characteristics.

Surface area	411 ha	1,015 ac
Lake volume	12,450,747 m ³	10,094 ac-ft
Mean depth	3.1 m	17 ft
Summer residence time (2019)		1.42 y

Table 2. Measured hydrologic characteristics - 1 June to 30 September, 2019.		
Variable		(m ³ /d)
Δ Pool storage		3,793
Hydrological inputs	Direct precipitation	18,132
	Straight River	24,090
	Sum	42,222

Table 3. Straight River flow-averaged summer (Jun-Sep) total phosphorus (P) and soluble reactive P concentrations and loads in 2019.

Variable	Concentration (mg/L)	P loading	
		(kg/d)	(kg/summer)
Total P	0.068	1.81	221
Soluble P	0.031	0.83	101

Table 4. Mean limnological trophic state variables for Big Round Lake in 2019. Means were calculated for the period June-September unless otherwise noted. TSI = trophic state index.

Variable	Mean
Surface total P, mg/L (Jun - Sep)	0.077
Secchi transparency, m (Jun - Sep)	1.49
Secchi transparency, ft (Jun - Sep)	4.89
Chlorophyll, ug/L (Jun - Sep)	81.4
Chlorophyll, ug/L (Jul - Sep)	105.2
Carlson TSI-P (Jun - Sep)	67
Carlson TSI-SD (Jun - Sep)	54
Carlson TSI-CHLa (Jun - Sep)	74
Wisconsin TSI-P (Jun - Sep)	62
Wisconsin TSI-SD (Jun - Sep)	54
Wisconsin TSI-CHLa (Jun - Sep)	68

Table 5. Mean (n=3) laboratory-derived rates of diffusive P flux from sediment under anaerobic and aerobic conditions.		
Variable	Anaerobic	Aerobic
Rate (mg/m ² d)	0.92	0.35
1 Standard Error	0.12	0.08

Table 6. Estimated summer (Jun-Sep) watershed loading and internal P loading estimated from P mass balance, laboratory-derived diffusive P flux, and evaluation of a P concentration profile from the sediment.

Variable		(kg/summer)
Watershed P loading	Straight River	221
Internal P loading	P Mass balance	1202
	Laboratory diffusive P flux	217
	Sediment core P profile	328

Table 7. Estimation of internal P loading from sediment biologically-labile (i.e., subject to internal P loading and recycling) phosphorus concentrations (Rydin et al. 2011). Biologically-labile P is the sum of the loosely-bound P, iron-bound P, and labile organic P fractions.

Gross P deposition	494	kg/y
P burial rate	166	kg/y
Internal P loading rate	328	kg/y
P burial efficiency	34	%

Fig. 1. Bathymetric map of Big Round Lake. Red dot denotes the lake sampling station.

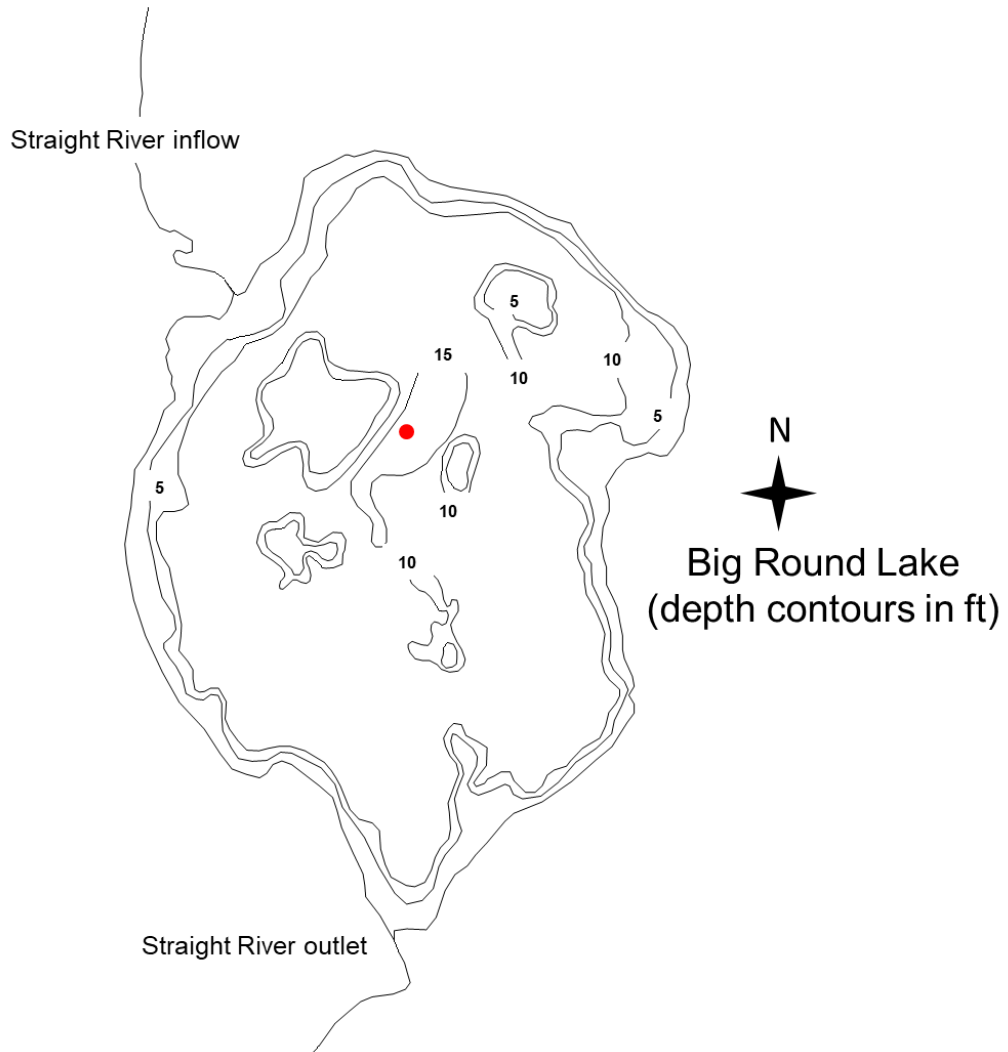




Fig. 2. Straight River above Big Round Lake at 250th Ave showing bridge construction and boom line.

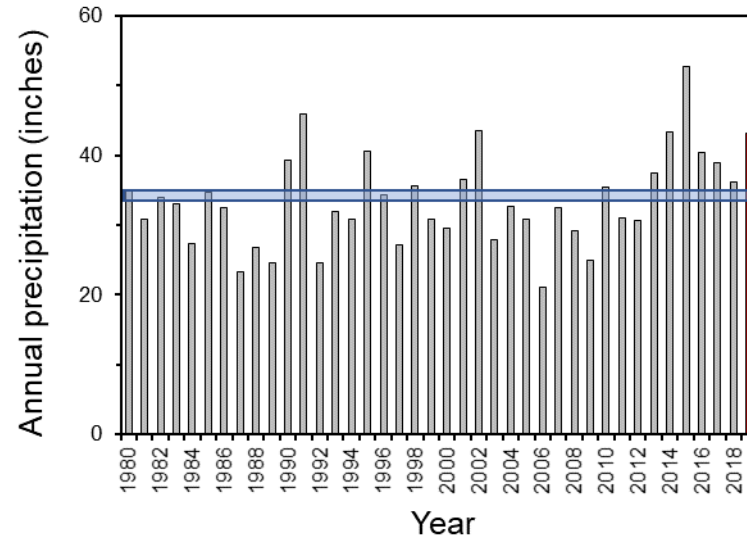


Fig. 3. Variations in annual precipitation measured at Amery Wisconsin. Red bar represents 2019. Horizontal blue line denotes average precipitation since 1980.

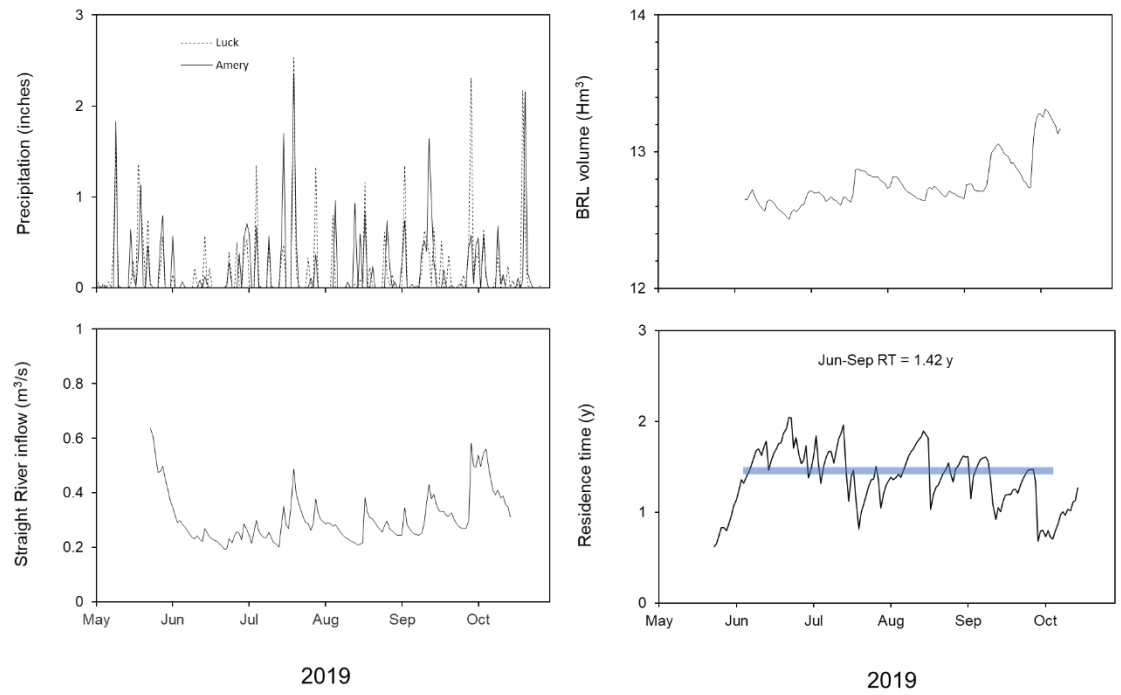
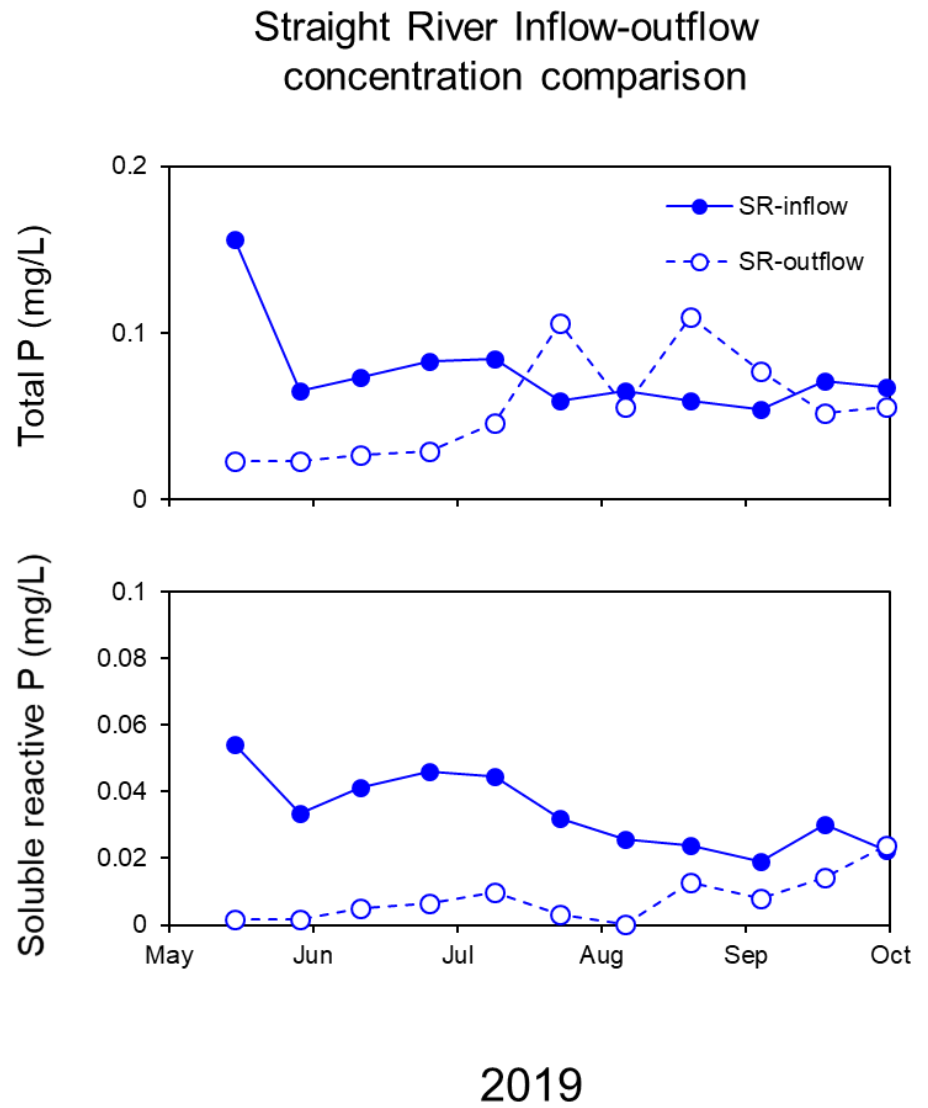


Fig. 4. Seasonal variations in daily precipitation measured at Amery and Luck Wisconsin (upper left), the Straight River inflow (lower left), Big Round Lake (BRL) volume (upper right), and residence time (lower right) during the summer of 2019.

Fig. 5. Seasonal variations in total phosphorus (P) and soluble reactive P at the Straight River (SR) inflow and outflow station.



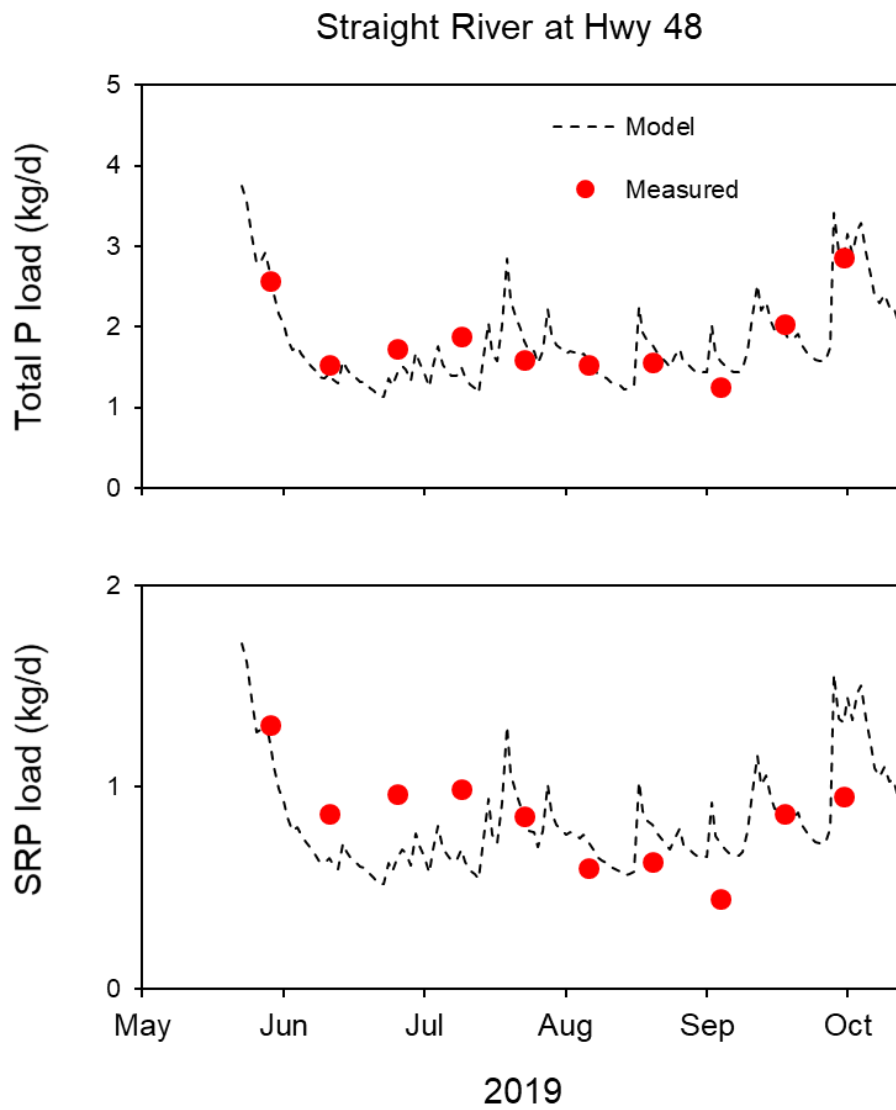
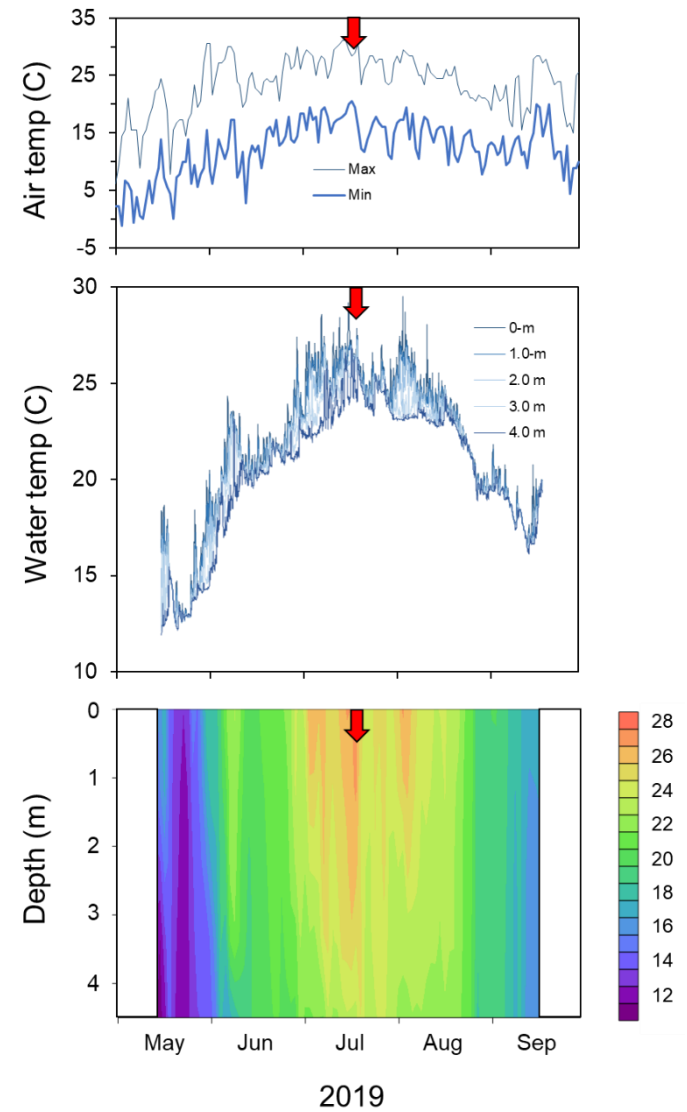


Fig. 6. Seasonal variations in modeled (i.e., FLUX) and measured total phosphorus (P) and soluble reactive P (SRP) loads from the Straight River entering Big Round Lake in 2019.

Fig. 7. Seasonal variations in daily air temperature minimum and maximum (upper panel), hourly water temperature measured at 1-m depth intervals (middle panel), and temperature contours (lower panel) at the sampling station located in Big Round Lake 2019. Red arrows denote the time of tornados in the area (19 July).



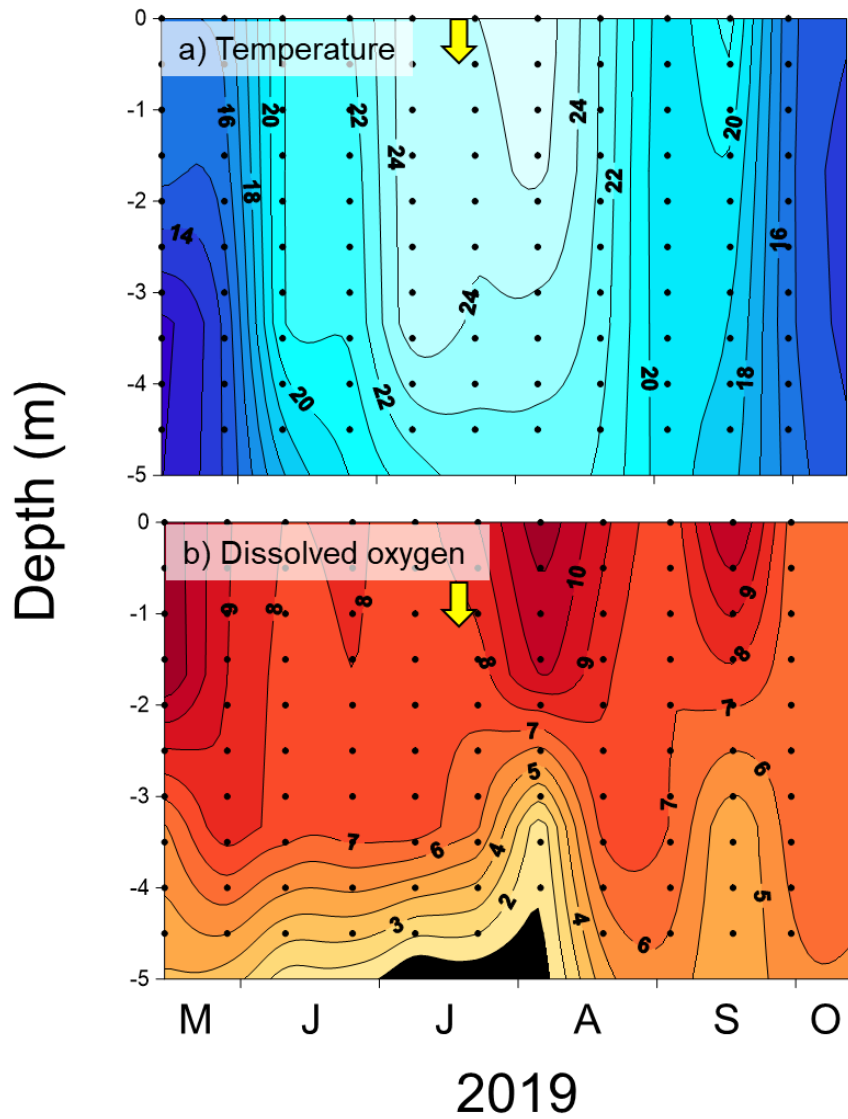


Fig. 8. Seasonal and vertical variations in water temperature (upper panel) and dissolved oxygen (lower panel) at the Big Round Lake sampling station in 2019. Yellow arrows denote the time of tornados in the area (19 July). Black bottom area in the lower panel represents the period of hypolimnetic anoxia.

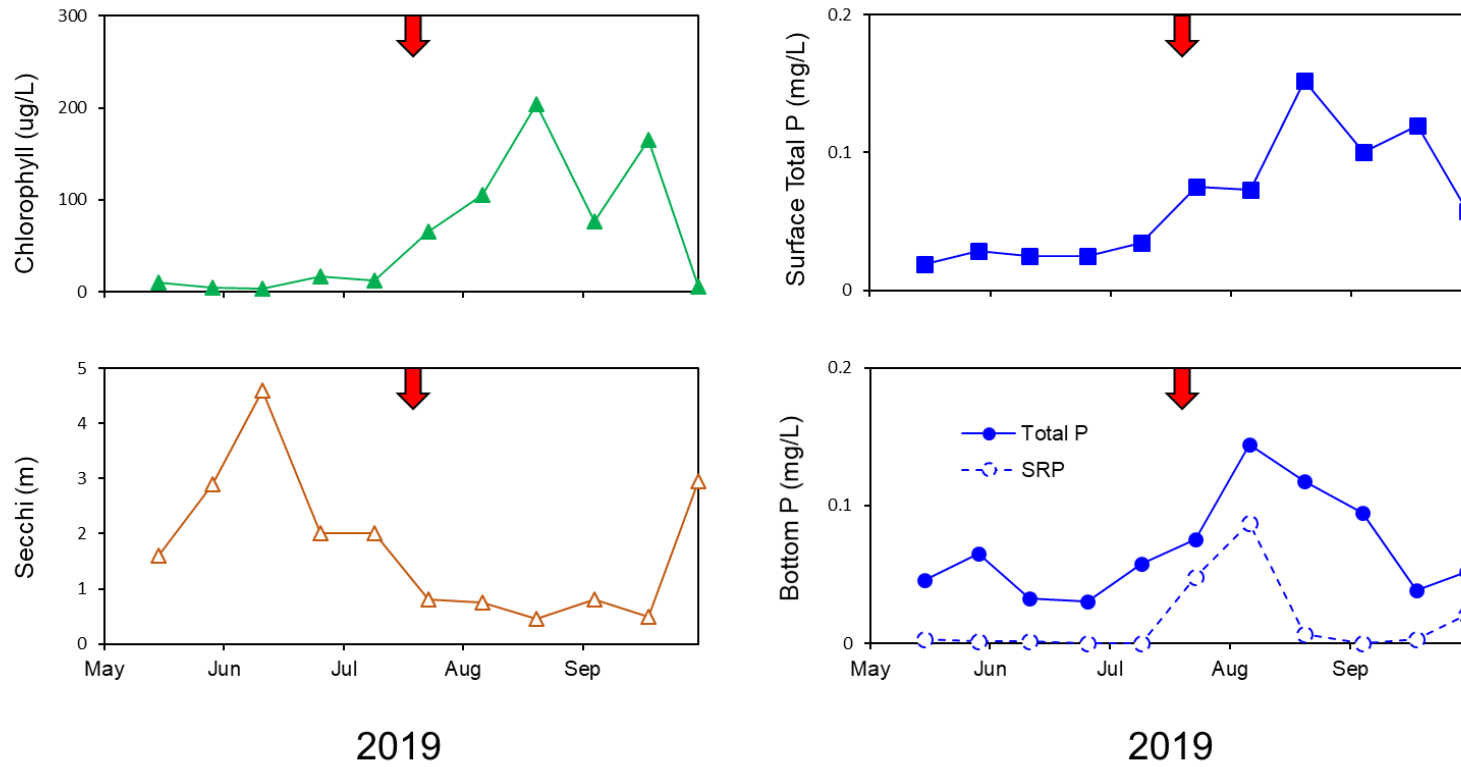


Fig. 9. Seasonal variations in chlorophyll (2-m integrated sample, upper left), Secchi transparency (lower left), total phosphorus (P) in the upper 2-m water column (upper right), and total P and soluble reactive P (SRP) concentrations in the hypolimnion above the sediment

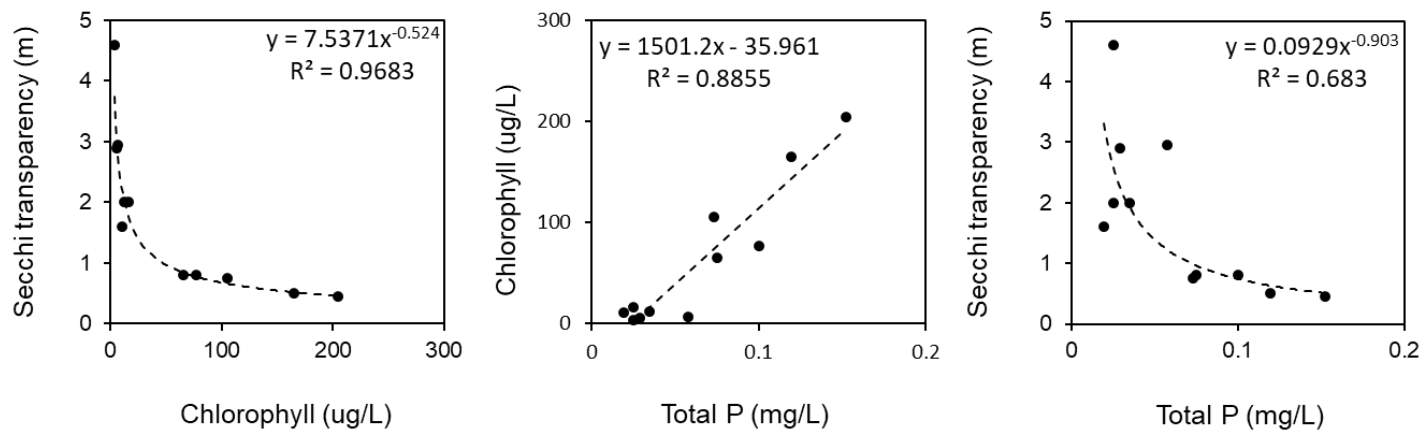


Fig. 10. Relationships between limnological trophic state variables.

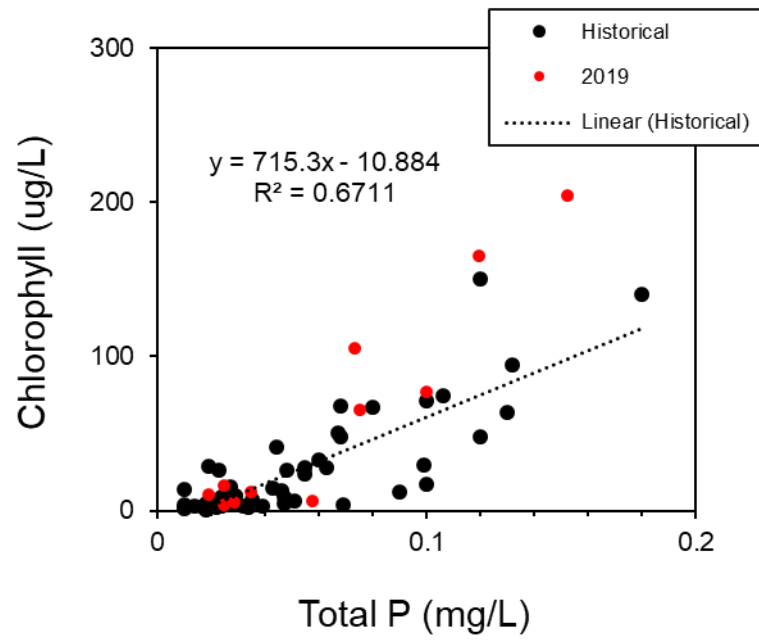


Fig. 11. Total phosphorus (P) versus chlorophyll regression relationships comparison between historical and 2019.

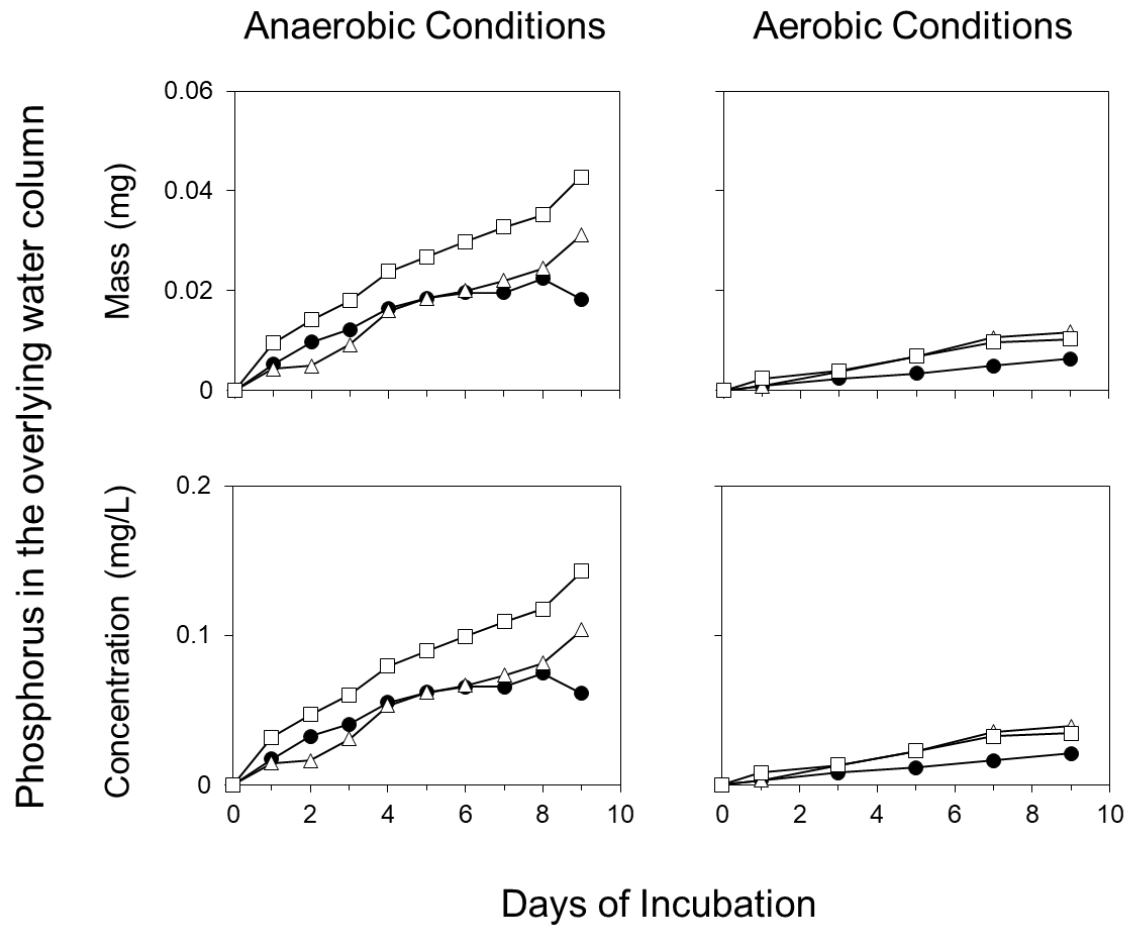


Fig. 12. Changes in soluble reactive phosphorus mass and concentration versus days of incubation in replicate sediment core incubation systems subjected to anaerobic or aerobic conditions.

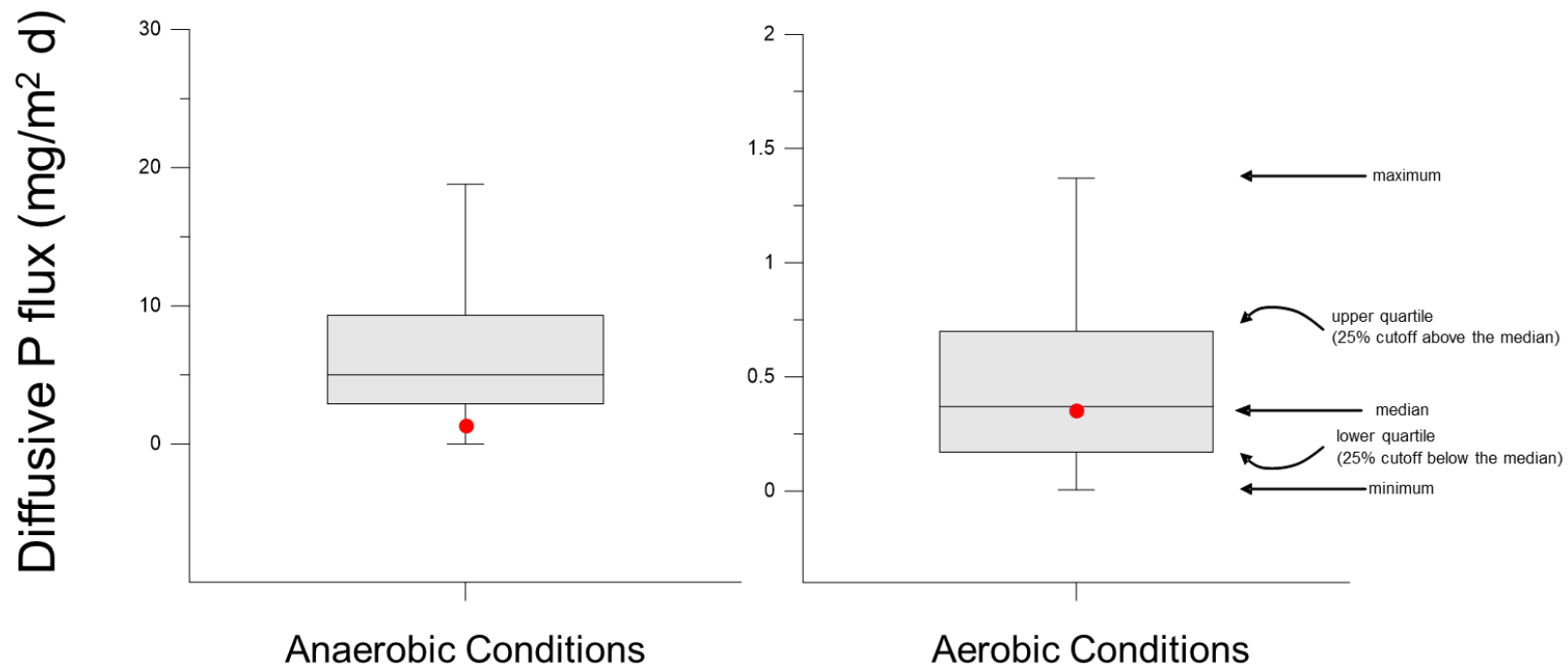


Fig. 13. Box and whisker plot comparing laboratory-derived diffusive P flux from sediment collected in Big Round Lake (red circle) with other lake sediment in the region.

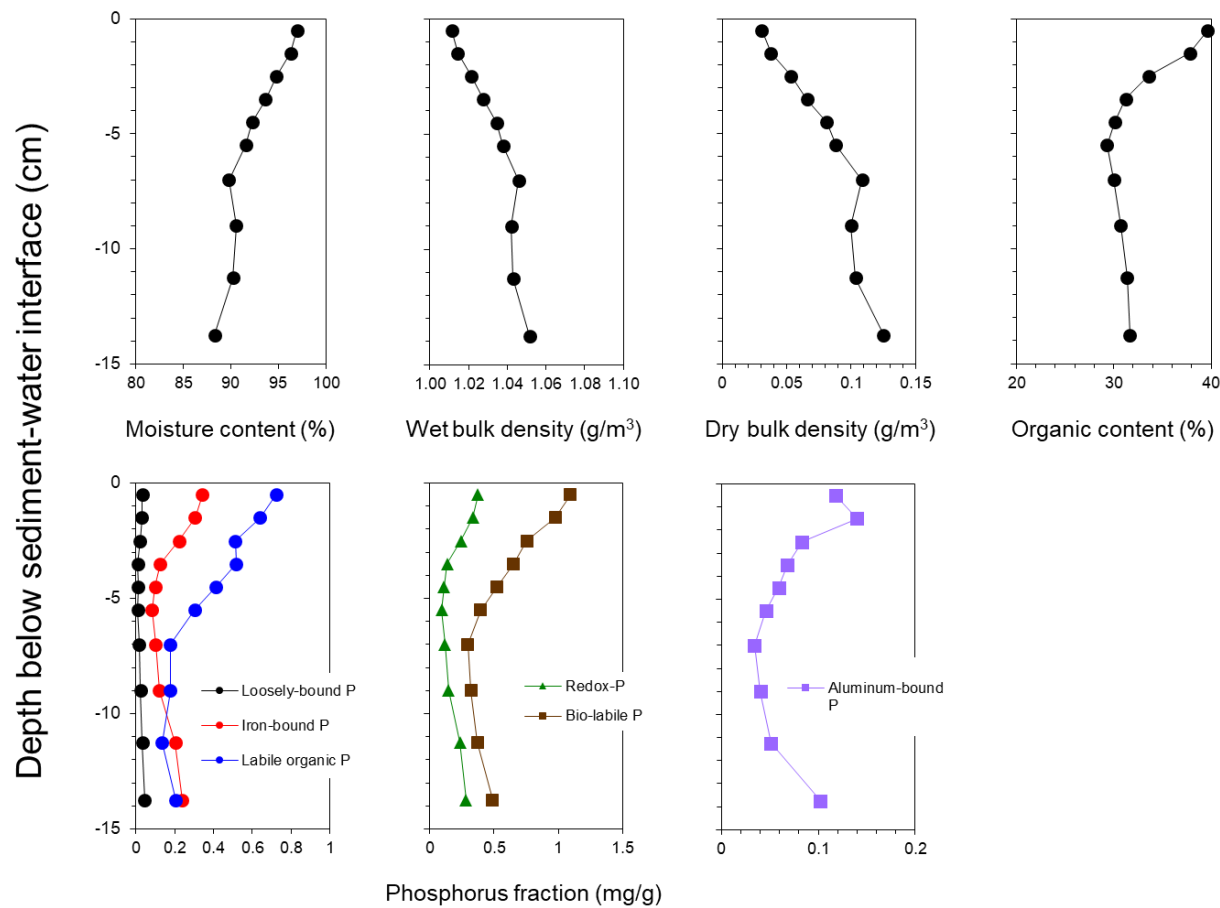


Fig.14. Sediment core vertical profiles of physical-textural characteristics and phosphorus fractions.

*Biologically-labile
phosphorus*

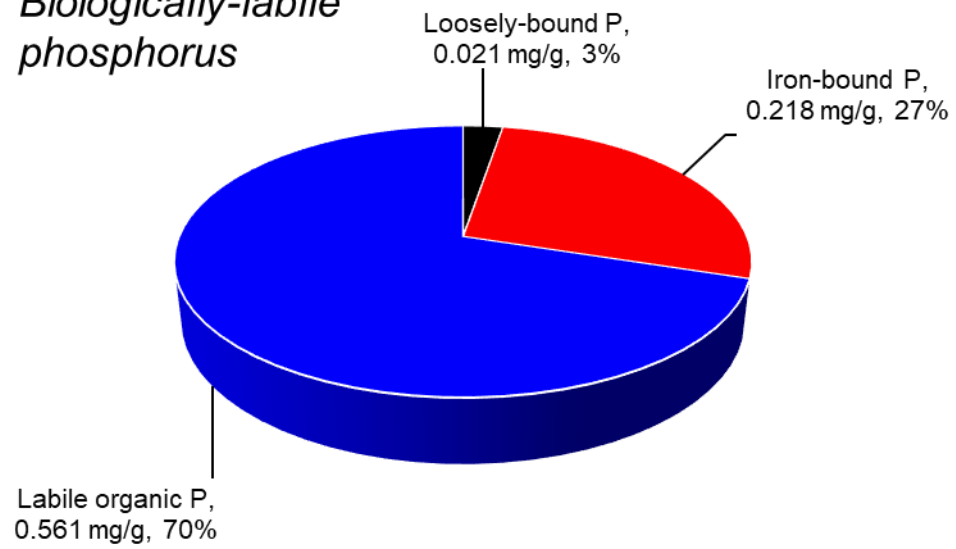


Fig. 15. Percent composition of the biologically-labile phosphorus fraction in the upper 5-cm on sediment collected in Big Round Lake.

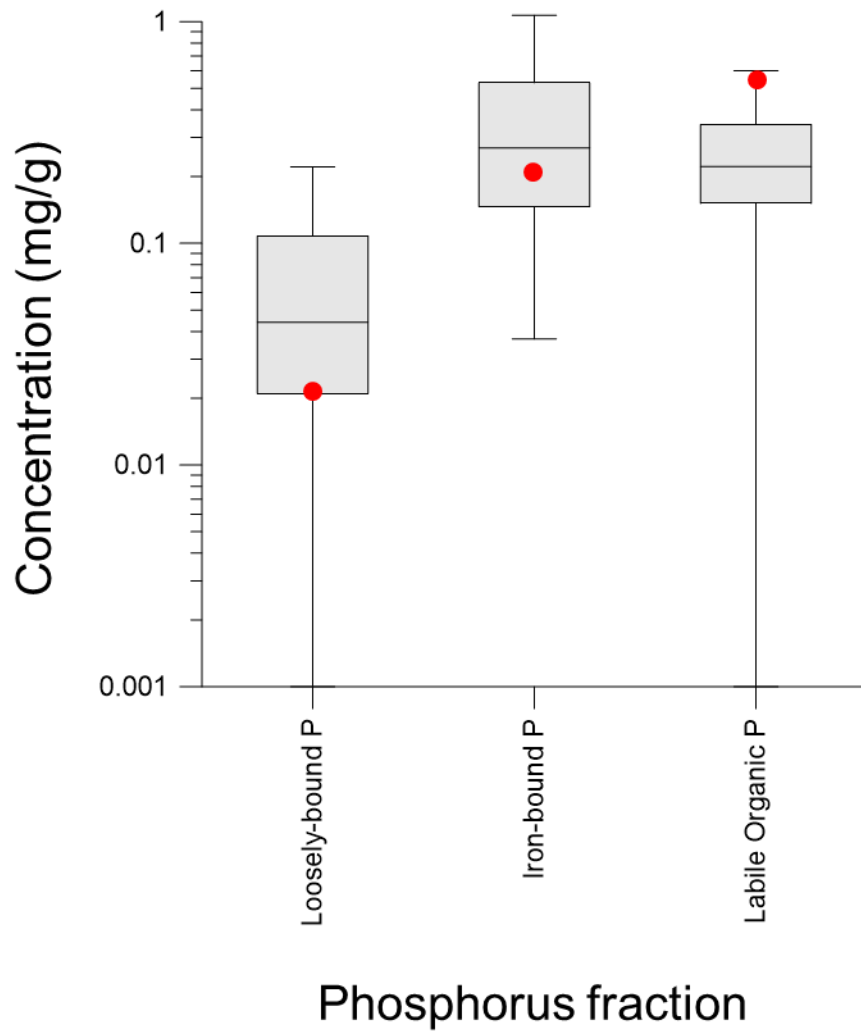


Fig. 16. Box and whisker plot comparing concentrations of loosely-bound, iron-bound, and labile organic phosphorus (P) from the upper 5-cm sediment layer in Big Round Lake (red circles) with other lake sediment concentrations in the region.

Fig. 17. Box and whisker plot comparing concentrations of redox-sensitive and biologically-labile phosphorus (P) from the upper 5-cm sediment in Big Round Lake (red circles) with other lake sediment concentrations in the region.

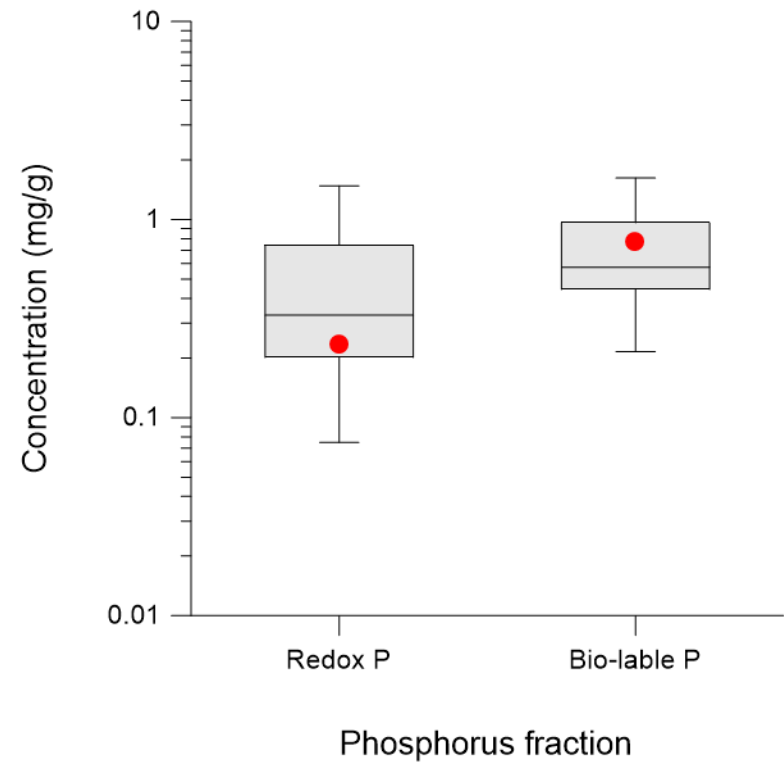
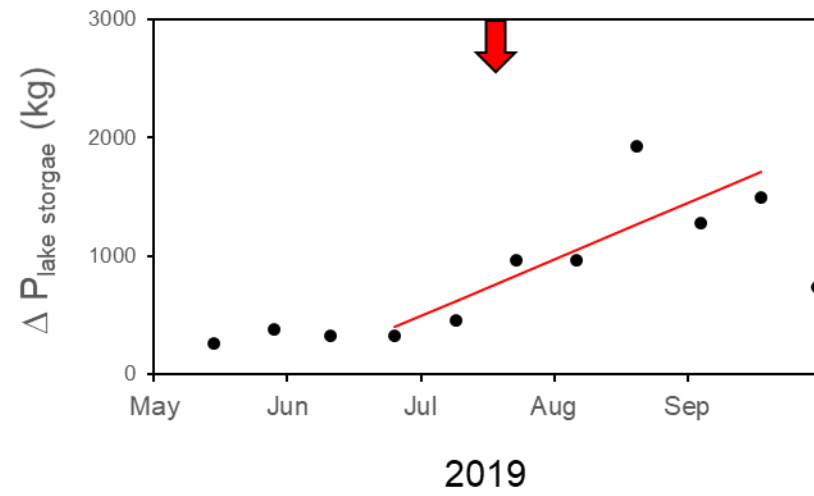


Fig. 18. Seasonal changes in Big Round Lake total phosphorus (P) mass in 2019. Red arrow denotes the period of tornado touchdowns in the area.



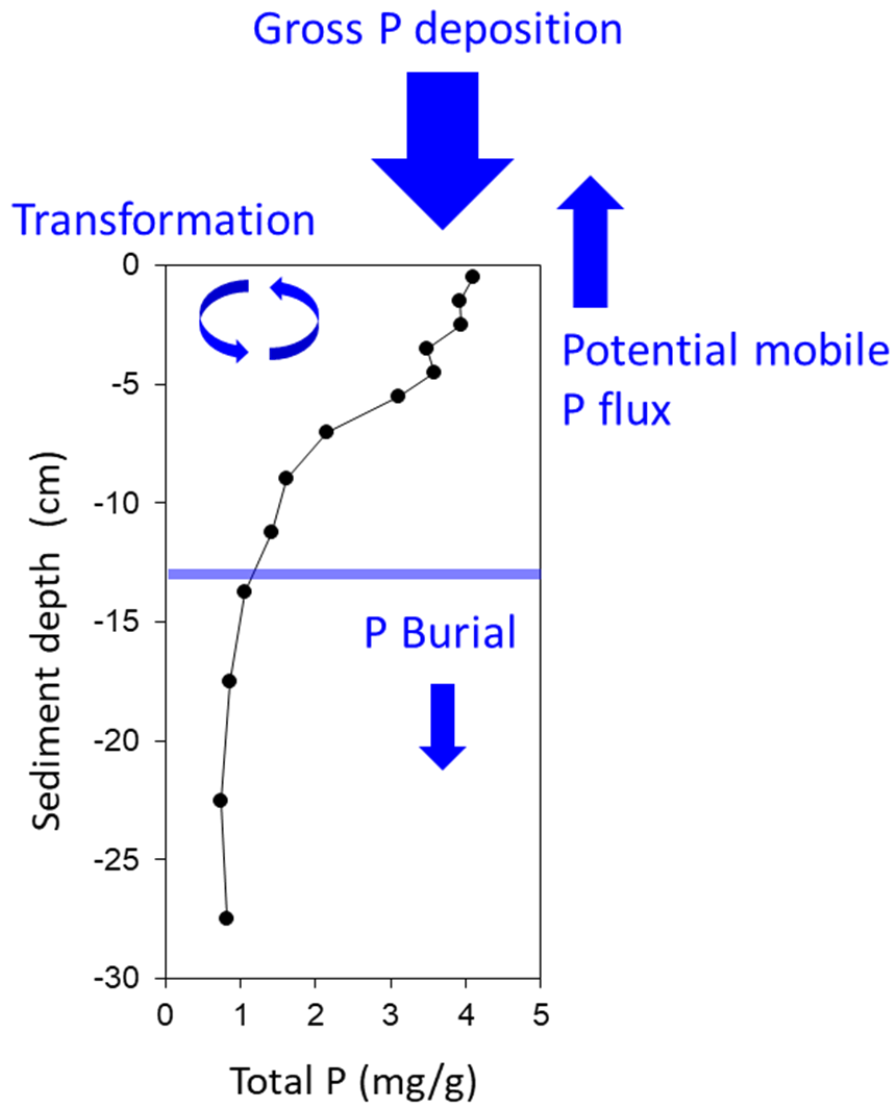
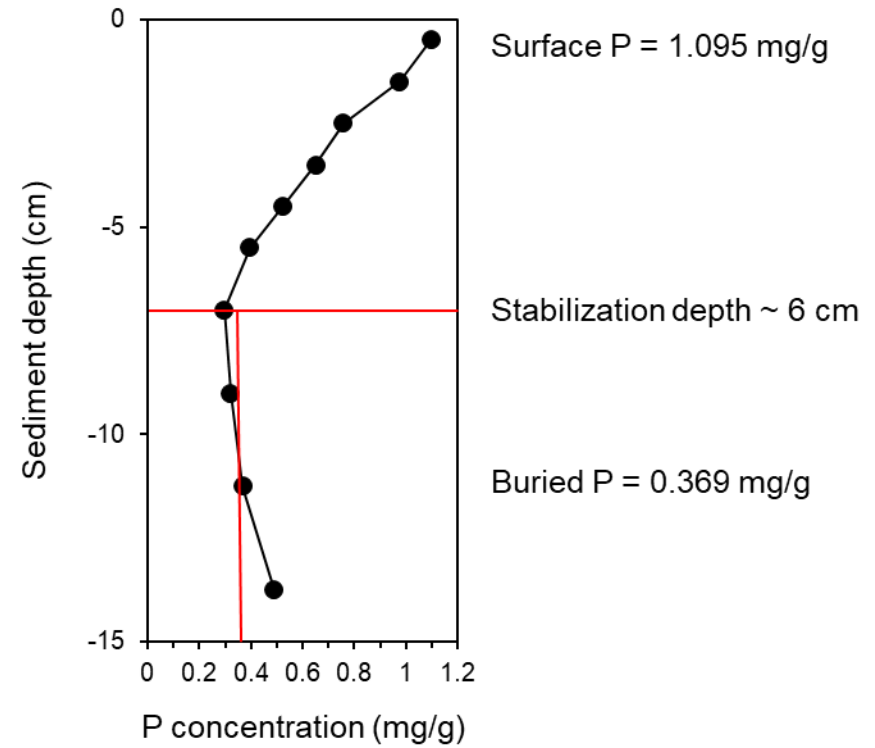


Fig. 19. Conceptual diagram relating vertical variations in sediment phosphorus (P) concentration and the sediment P surface bulge to gross P deposition, P burial, and internal P loading.

Fig. 20. Vertical variations in biologically-labile P concentrations.

Biologically-labile P



2019 Summer P Loads

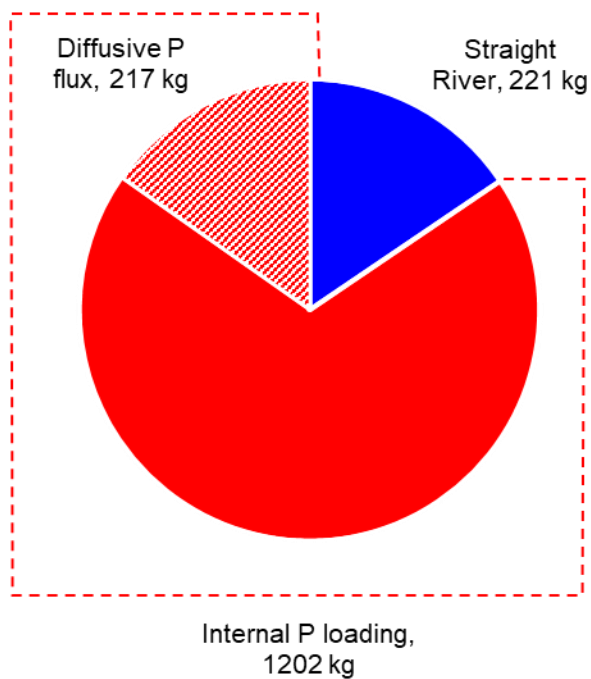


Fig. 21. Comparison of measured summer phosphorus (P) loads to Big Round Lake in 2019. Internal P loading, estimated from P mass balance, accounted for 84% of the measured P loading versus only 16% input from the Straight River watershed. Diffusive P flux only accounted for 23% of the internal P loading calculated using P mass balance.